

Boundary Element Approximation for Maxwell's Eigenvalue Problem

C. Wieners

J. Xin

Preprint Nr. 12/02

INSTITUT FÜR WISSENSCHAFTLICHES RECHNEN
UND MATHEMATISCHE MODELLBILDUNG



Anschriften der Verfasser:

Prof. Dr. Christian Wieners
Institut für Angewandte und Numerische Mathematik
Karlsruher Institut für Technologie (KIT)
D-76128 Karlsruhe

Dr. Jiping Xin
State Key Laboratory of Scientific and Engineering Computing, AMSS
Chinese Academy of Sciences
ZhongGuanCun Donglu 55
100190 Beijing
China

Boundary Element Approximation for Maxwell's Eigenvalue Problem

Christian Wieners

*Fakultät für Mathematik, Karlsruhe Institute of Technology (KIT),
Kaiserstr. 12, 76128 Karlsruhe, Germany*

Jiping Xin

*State Key Laboratory of Scientific and Engineering Computing, AMSS,
Chinese Academy of Sciences, ZhongGuanCun Donglu 55, 100190 Beijing, China*

Abstract

We introduce a new method for computing eigenvalues of the Maxwell operator with boundary finite elements. On bounded domains with piecewise constant material coefficients, the Maxwell solution for fixed wave number can be represented by boundary integrals, which allows to reduce the eigenvalue problem to a nonlinear problem for determining the wave number along with boundary and interface traces. A Galerkin discretization yields a smooth nonlinear matrix eigenvalue problem which is solved by Newton's method or, alternatively, the contour integral method. Several numerical results including an application to the band structure computation of a photonic crystal illustrate the efficiency of this approach.

1. Introduction

The boundary element method is a well established discretization for indefinite Helmholtz problems which allows to reduce volume computations to surface computations. This is a severe reduction of degrees of freedom. On the other hand, the resulting Galerkin matrices are dense (if no reduction technique is applied) and the assembling requires the integration of strongly singular functions. Thus, it is quite challenging to realize this method efficiently.

In principle, the boundary element method applies to a broad class of linear operators with constant coefficients, as long as a fundamental solution

is available. For Maxwell's equations the fundamental solution, a representation formula, and a corresponding boundary integral equation is well-known and for smooth boundaries classical techniques can be used. Nevertheless, a weak formulation for Lipschitz domains requires a careful analysis of the underlying trace spaces, and the full analysis of a Galerkin boundary element method is quite involved (see [4] for an overview).

Eigenvalues of the Maxwell operator are wave numbers for which a non-trivial solution for the problem with homogeneous right-hand side exists. This results into a nonlinear (in fact holomorphic) eigenvalue problem. The boundary element approach for the computation of eigenvalues was recently proposed for the Helmholtz case by Steinbach and Unger [15, 16, 17] using a Newton method. Based on the theory of holomorphic operator functions, they provide a full convergence analysis which shows cubic convergence for lowest order boundary element discretizations.

Alternatively, the contour integral method can be applied to compute directly all eigenvalues within a prescribed complex set. Following the algorithmic approach proposed in [1], the resolvent and its first moment are integrated numerically along a smooth closed curve in the complex plane. This allows to recover the singular points of the resolvent via the residual formula.

Both methods are applied to the Maxwell problem in a single domain. For the application to coupled problems with different coefficients in every subdomain, we transfer the coupling method proposed by Langer et. al. in [11] to the Maxwell system. For this purpose the two equations in the Calderon projection for each subdomain together with the interface conditions are combined to a self-adjoint problem for the Dirichlet and Neumann traces on the interfaces. In discrete form, this leads again to a nonlinear matrix eigenvalue problem.

The paper is organized as follows. We start with a review on the boundary element method for Maxwell's equations in bounded domains with constant coefficients and fixed wave number. Then, a domain decomposition formulation is introduced. Next, we consider the eigenvalue problem as a nonlinear equation to find wave numbers which allow for nontrivial homogeneous solutions. Finally, this is transferred to piecewise constant coefficients via domain decomposition. For all problems we present numerical results, where—for comparison—the eigenvalues are also computed with a standard finite element approach.

2. The Maxwell boundary value problem

We start with a review on Maxwell's equations, and then we define the appropriate function spaces for a weak boundary integral setting summarizing the results from [5, 6, 3, 2], where we mainly follow the overview given by Buffa and Hiptmair in [4].

2.1. Maxwell's equations in linear isotropic materials

Let $\Omega \subset \mathbb{R}^3$ be a bounded Lipschitz domain with piecewise smooth boundary $\Gamma = \partial\Omega$. We consider Maxwell's equations in linear isotropic materials: determine the magnetic field \mathbf{H} and the electric field \mathbf{E} such that

$$\begin{aligned} \mu\partial_t\mathbf{H} + \nabla \times \mathbf{E} &= \mathbf{0}, & \epsilon\partial_t\mathbf{E} - \nabla \times \mathbf{H} &= \mathbf{0}, \\ \nabla \cdot \mathbf{E} &= 0, & \nabla \cdot \mathbf{H} &= 0, \end{aligned}$$

where we assume constant permittivity $\epsilon > 0$ and permeability $\mu > 0$. Special solutions of this equation can be obtained by the ansatz for monochromatic waves $\mathbf{E}(t, x) = \exp(-i\omega t)\mathbf{u}(x)$ with frequency ω , which yields

$$\nabla \times (\nabla \times \mathbf{u}) - k^2\mathbf{u} = \mathbf{0} \quad \text{and} \quad \nabla \cdot \mathbf{u} = 0 \quad (1)$$

with the wave number $k = \omega\sqrt{\epsilon\mu}$. If k^2 is not an eigenvalue of the homogeneous Dirichlet problem with $\mathbf{n} \times \mathbf{u} = \mathbf{0}$ on Γ , the solution of (1) is uniquely determined by Dirichlet values

$$\mathbf{n} \times \mathbf{u} = \mathbf{f} \quad \text{on } \Gamma.$$

On the other hand, if k^2 is not an eigenvalue of the homogeneous Neumann problem with $\mathbf{n} \times (\nabla \times \mathbf{u}) = \mathbf{0}$ on Γ , a unique solution of (1) for given Neumann values

$$\mathbf{n} \times (\nabla \times \mathbf{u}) = \mathbf{g} \quad \text{on } \Gamma$$

exists. Since we consider the case that the boundary Γ is only piecewise smooth, the boundary conditions hold—even for smooth solutions—only almost everywhere on Γ .

The main observation for the boundary integral formulation is that the solution \mathbf{u} of the Maxwell problem (1) can be reconstructed if both boundary data—the Dirichlet values \mathbf{f} and the Neumann values \mathbf{g} —are known.

2.2. The representation formula for Maxwell's equations

The starting point to derive the representation formula is the fundamental solution for the Helmholtz equation

$$E_k(x, y) = \frac{\exp(ik|x - y|)}{4\pi|x - y|}$$

satisfying $-(\Delta_x + k^2)E_k(x, y) = \delta(x - y)$ in distributional sense. Then, we find that $\mathbf{G}_k(x, y) = E_k(x, y)\mathbf{I} + k^{-2}\nabla_x(\nabla_y E_k(x, y))^T$ is a fundamental solution for Maxwell's equations. Since the fundamental solution is complex, all function spaces in this section will be complex-valued. Nevertheless, in many cases the actual computation can be reduced to the real part.

Integrating the fundamental solution E_k along the boundary Γ with boundary data v defines the single-layer potential

$$\tilde{V}_k(v)(x) = \int_{\Gamma} E_k(x, y)v(y) ds_y \quad x \in \Omega,$$

and we observe that $\tilde{V}_k(v)$ solves the homogeneous Helmholtz problem in Ω . The corresponding vectorial single-layer potential for given boundary data $\mathbf{v} = (v_1, v_2, v_3)$ is denoted by $\tilde{\mathbf{V}}_k(\mathbf{v}) = (\tilde{V}_k(v_1), \tilde{V}_k(v_2), \tilde{V}_k(v_3))$.

In the same way we obtain the Maxwell single-layer potential by integrating the fundamental solution \mathbf{G}_k along the boundary

$$\begin{aligned} \Psi_{\text{SL}}^k(\mathbf{v})(x) &= - \int_{\Gamma} \mathbf{G}_k(x, y)\mathbf{v}(y) ds_y \\ &= -\tilde{\mathbf{V}}_k(\mathbf{v})(x) - \frac{1}{k^2}\nabla_x \tilde{V}_k(\text{div}_{\Gamma} \mathbf{v})(x) \\ &= - \int_{\Gamma} E_k(x, y)\mathbf{v}(y) ds_y - \frac{1}{k^2}\nabla_x \int_{\Gamma} E_k(x, y) \text{div}_{\Gamma}(\mathbf{v}(y)) ds_y \end{aligned}$$

(observe the sign convention), and the Maxwell double-layer potential

$$\Psi_{\text{DL}}^k(\mathbf{w})(x) = -\nabla_x \times \tilde{\mathbf{V}}_k(\mathbf{w})(x) = -\nabla_x \times \int_{\Gamma} E_k(x, y)\mathbf{w}(y) ds_y, \quad x \in \Omega$$

where \mathbf{v}, \mathbf{w} are tangential boundary data with $\mathbf{v} \cdot \mathbf{n} = \mathbf{w} \cdot \mathbf{n} = \mathbf{0}$ and where div_{Γ} is the adjoint to the surface gradient for tangential vector fields on Γ . Again, by construction the potentials $\Psi_{\text{SL}}^k(\mathbf{v})$ and $\Psi_{\text{DL}}^k(\mathbf{w})$ are solutions of

the homogeneous Maxwell's equations (1). For smooth solutions \mathbf{u} , using Green's first and second formulae, the representation formula

$$\mathbf{u}(x) = \Psi_{\text{SL}}^k(\mathbf{n} \times (\nabla \times \mathbf{u}))(x) + \Psi_{\text{DL}}^k(\mathbf{n} \times \mathbf{u})(x) \quad x \in \Omega, \quad (2)$$

can be derived, cf. [9, Sect. 6.2] and [4, Sect. 4].

2.3. Trace operators and function spaces

Let Γ be composed of smooth manifolds Γ_j with exterior normals \mathbf{n}_j such that $\Gamma = \bigcup_j \bar{\Gamma}_j$ and $\Gamma_j \cap \Gamma_m = \emptyset$, $j \neq m$. Dirichlet and Neumann trace operators are defined for smooth vector fields \mathbf{v} in Ω and $x \in \Gamma_j$ by

$$\gamma_{\mathbf{t}}(\mathbf{v})(x) = \lim_{\tilde{x} \in \Omega \rightarrow x \in \Gamma_j} \mathbf{n}_j(x) \times \mathbf{v}(\tilde{x}), \quad \gamma_{\mathbf{N}}^k(\mathbf{v})(x) = \frac{1}{k} \gamma_{\mathbf{t}}(\nabla \times \mathbf{v})(x).$$

Note that we include the dependence of k in the Neumann trace only to obtain symmetry in the Calderon operator below.

Let $e_{jm} = \partial\Gamma_j \cap \partial\Gamma_m$ be a boundary edge with a tangent \mathbf{t}_{jm} , and let $\mathbf{n}_{\partial\Gamma_j} \in \text{affine}(\Gamma_j)$ be the tangential normal along $\partial\Gamma_j$, i.e., $\mathbf{n}_{\partial\Gamma_j} = \mathbf{n}_j \times \mathbf{t}_{jm}$ on the edge e_{jm} . From the identity

$$\gamma_{\mathbf{t}}(\mathbf{v})|_{\bar{\Gamma}_j} \cdot \mathbf{n}_{\partial\Gamma_j} = (\mathbf{n}_j \times \mathbf{v}|_{\bar{\Gamma}_j}) \cdot (\mathbf{n}_j \times \mathbf{t}_{jm}) = \mathbf{t}_{jm} \cdot \mathbf{v}|_{\bar{\Gamma}_j} \quad \text{on } e_{jm} \quad (3)$$

we obtain for smooth vector fields \mathbf{v} and functions w

$$\sum_j \int_{\partial\Gamma_j} \gamma_{\mathbf{t}}(\mathbf{v})|_{\bar{\Gamma}_j} \cdot \mathbf{n}_{\partial\Gamma_j} w \, dl = \sum_{j \neq m} \int_{e_{jm}} \mathbf{t}_{jm} \cdot \mathbf{v}|_{\bar{\Gamma}_j} w \, dl = 0 \quad (4)$$

since $\mathbf{t}_{jm} = -\mathbf{t}_{mj}$. For smooth functions w in $\bar{\Omega}$, we define a.e. the tangential gradient $\nabla_{\Gamma} w = \nabla w - (\mathbf{n} \cdot \nabla w) \mathbf{n} \in \mathbf{L}_{\mathbf{t}}^{\infty}(\Gamma) := \{\mathbf{h} \in \mathbf{L}^{\infty}(\Gamma) : \mathbf{h} \cdot \mathbf{n} = 0\}$ on the boundary. Then, Green's formula in Ω , Gauss formula on Γ_j , and the identity (4) together yield

$$\begin{aligned} \int_{\Omega} \nabla \times \mathbf{v} \cdot \nabla w \, dx &= \int_{\partial\Omega} (\mathbf{n} \times \mathbf{v}) \cdot \nabla w \, ds = \sum_j \int_{\Gamma_j} \gamma_{\mathbf{t}}(\mathbf{v}) \cdot \nabla_{\Gamma} w \, ds \\ &= \sum_j \left(\int_{\partial\Gamma_j} \gamma_{\mathbf{t}}(\mathbf{v})|_{\bar{\Gamma}_j} \cdot \mathbf{n}_{\partial\Gamma_j} w \, dl - \int_{\Gamma_j} \text{div}_{\Gamma} \gamma_{\mathbf{t}}(\mathbf{v}) w \, ds \right) \\ &= - \int_{\Gamma} \text{div}_{\Gamma} \gamma_{\mathbf{t}}(\mathbf{v}) w \, ds. \end{aligned} \quad (5)$$

Now, we extend these definitions from smooth functions to distributions. For $\mathbf{v} \in \mathbf{H}(\mathbf{curl}, \Omega)$ the weak Dirichlet trace operator $\gamma_{\mathbf{t}}(\mathbf{v}) \in \mathbf{H}^{-1/2}(\Gamma)$ is defined by

$$\langle \gamma_{\mathbf{t}}(\mathbf{v}), \mathbf{w}|_{\Gamma} \rangle = \int_{\Omega} \nabla \times \mathbf{v} \cdot \mathbf{w} \, dx - \int_{\Omega} \mathbf{v} \cdot \nabla \times \mathbf{w} \, dx, \quad \mathbf{w} \in \mathbf{C}^{\infty}(\bar{\Omega}). \quad (6)$$

Then, extending the equation (5) to $\mathbf{v} \in \mathbf{H}(\mathbf{curl}, \Omega)$ shows that in distributional sense $\operatorname{div}_{\Gamma} \gamma_{\mathbf{t}}(\mathbf{v}) \in \mathbf{H}^{-1/2}(\Gamma)$ is defined by

$$\langle \operatorname{div}_{\Gamma} \gamma_{\mathbf{t}}(\mathbf{v}), w|_{\Gamma} \rangle = - \int_{\Omega} \nabla \times \mathbf{v} \cdot \nabla w \, dx, \quad w \in C^{\infty}(\bar{\Omega}).$$

In particular, this gives for the trace space

$$\mathbf{W}^{-1/2}(\Gamma) = \gamma_{\mathbf{t}}(\mathbf{H}(\mathbf{curl}, \Omega)) \subset \mathbf{H}^{-1/2}(\Gamma)$$

that $\operatorname{div}_{\Gamma} \mathbf{W}^{-1/2}(\Gamma) \subset \mathbf{H}^{-1/2}(\Gamma)$ is well-defined. This property indeed characterizes the trace space, i.e., $\mathbf{W}^{-1/2}(\Gamma) = \{\mathbf{v} \in \mathbf{H}^{-1/2}(\Gamma) : \operatorname{div}_{\Gamma} \mathbf{v} \in \mathbf{H}^{-1/2}(\Gamma) \text{ and } \mathbf{v} \cdot \mathbf{n} = 0\}$, cf. [3].

Finally, we define the anti-linear pairing

$$\langle \mathbf{v}, \mathbf{w} \rangle_{\tau, \Gamma} = \int_{\Gamma} (\mathbf{v} \times \mathbf{n}) \cdot \bar{\mathbf{w}} \, ds, \quad \mathbf{v}, \mathbf{w} \in \mathbf{L}_{\mathbf{t}}^2(\Gamma), \quad (7)$$

and we observe again from Green's first formula that this pairing extends to $\mathbf{v} \in \mathbf{H}(\mathbf{curl}^2, \Omega)$ and $\mathbf{w} \in \mathbf{H}(\mathbf{curl}, \Omega)$ by

$$\langle \gamma_{\mathbf{N}}^k(\mathbf{v}), \gamma_{\mathbf{t}}(\mathbf{w}) \rangle_{\tau, \Gamma} = \frac{1}{k} \int_{\Omega} (\nabla \times \nabla \times \mathbf{v} \cdot \bar{\mathbf{w}} - \nabla \times \mathbf{v} \cdot \nabla \times \bar{\mathbf{w}}) \, dx.$$

2.4. Boundary integral operators

For smooth functions v in Ω we define the Dirichlet and Neumann traces for $x \in \Gamma_j$ by

$$\gamma_0(v)(x) = \lim_{\tilde{x} \in \Omega \rightarrow x \in \Gamma_j} v(\tilde{x}), \quad \gamma_1(v)(x) = \lim_{\tilde{x} \in \Omega \rightarrow x \in \Gamma_j} \nabla v(\tilde{x}) \cdot \mathbf{n}(x).$$

The single-layer potential operator \tilde{V}_k is well-defined from $\mathbf{H}^{-1/2}(\Gamma)$ to $\mathbf{H}^1(\Omega)$ [14, Sect. 6.9]. This shows that the potential operators Ψ_{SL}^k and Ψ_{DL}^k are also well-defined on $\mathbf{W}^{-1/2}(\Gamma)$ [4, Thm. 5]. For $\mathbf{v} \in \mathbf{W}^{-1/2}(\Gamma)$ we have

$\gamma_{\mathbf{t}}(\Psi_{\text{SL}}^k(\mathbf{v})), \gamma_{\mathbf{t}}(\Psi_{\text{DL}}^k(\mathbf{v})) \in \mathbf{W}^{-1/2}(\Gamma)$ [4, Thm. 5 and Cor. 2], which allows to define the boundary operators \mathbf{S}_k and \mathbf{C}_k

$$\begin{aligned}\mathbf{S}_k &= \gamma_{\mathbf{t}} \Psi_{\text{SL}}^k: \mathbf{W}^{-1/2}(\Gamma) \rightarrow \mathbf{W}^{-1/2}(\Gamma), \\ \frac{1}{2} \mathbf{I} + \mathbf{C}_k &= \gamma_{\mathbf{t}} \Psi_{\text{DL}}^k: \mathbf{W}^{-1/2}(\Gamma) \rightarrow \mathbf{W}^{-1/2}(\Gamma).\end{aligned}$$

The definition of the operator \mathbf{C}_k includes the jump relation, which is the Maxwell counterpart of the jump relation for the single-layer potential operator \tilde{V}_k and the adjoint double-layer boundary operator

$$\gamma_{\mathbf{1}}(\tilde{V}_k(v))(x) = \frac{1}{2}v(x) + \text{p.v.} \int_{\Gamma} \gamma_{1,x}(E_k(x, y))v(y) \, ds_y \quad (8)$$

for a.a. $x \in \Gamma$ [14, Lem. 6.8]. Finally, note that we have the identities

$$\gamma_{\mathbf{t}} \Psi_{\text{SL}}^k = \gamma_{\mathbf{N}}^k \Psi_{\text{DL}}^k \quad \text{and} \quad \gamma_{\mathbf{t}} \Psi_{\text{DL}}^k = \gamma_{\mathbf{N}}^k \Psi_{\text{SL}}^k \quad (9)$$

[4, Sect.4], so we just need to consider the Dirichlet trace.

For the explicit evaluation of the boundary operators we use the following lemma, where we sketch the proof for convenience of the reader [4, Sect. 5].

Lemma 1. *For $\mathbf{v}, \mathbf{w} \in \mathbf{L}_t^\infty(\Gamma)$ with $\text{div}_\Gamma \mathbf{v}, \text{div}_\Gamma \mathbf{w} \in L^\infty(\Gamma)$ we have*

$$\begin{aligned}\langle \mathbf{S}_k(\mathbf{v}), \mathbf{w} \rangle_{\tau, \Gamma} &= \int_{\Gamma} \int_{\Gamma} \left(\frac{1}{k} \text{div}_\Gamma \mathbf{v}(y) \text{div}_\Gamma \overline{\mathbf{w}(x)} - k \mathbf{v}(y) \cdot \overline{\mathbf{w}(x)} \right) E_k(x, y) \, ds_y ds_x, \\ \langle \mathbf{C}_k(\mathbf{w}), \mathbf{v} \rangle_{\tau, \Gamma} &= - \int_{\Gamma} \int_{\Gamma} \nabla_x E_k(x, y) \cdot (\mathbf{w}(y) \times \overline{\mathbf{v}(x)}) \, ds_y ds_x.\end{aligned}$$

Proof. For smooth vector fields \mathbf{v} , the definition of the potential Ψ_{SL}^k and the tangential trace yields for a.a. $x \in \Gamma$

$$\begin{aligned}\mathbf{S}_k(\mathbf{v})(x) &= -k \int_{\Gamma} \mathbf{n}(x) \times (E_k(x, y) \mathbf{v}(y)) \, ds_y \\ &\quad - \frac{1}{k} \text{p.v.} \int_{\Gamma} \mathbf{n}(x) \times \nabla_x (\text{div}_\Gamma(\mathbf{v}(y)) E_k(x, y)) \, ds_y.\end{aligned}$$

Now, inserting (7), the vector identity $(\mathbf{n} \times (\mathbf{w} \times \mathbf{n})) \cdot \mathbf{v} = \mathbf{w} \cdot \mathbf{v} - (\mathbf{n} \cdot \mathbf{w})(\mathbf{n} \cdot \mathbf{v})$ and integration by parts yields the first assertion. The definition of \mathbf{C}_k and the jump relation (8) directly yields for a.a. $x \in \Gamma$

$$\mathbf{C}_k(\mathbf{w})(x) = - \text{p.v.} \int_{\Gamma} \mathbf{n}(x) \times \nabla_x \times (E_k(x, y) \mathbf{w}(y)) \, ds_y.$$

Inserting (7) and the vector identity above gives the assertion. \square

2.5. *The weak formulation of the Maxwell boundary value problem*

The Calderon operator $\mathcal{C}: \mathbf{W}^{-1/2}(\Gamma) \times \mathbf{W}^{-1/2}(\Gamma) \rightarrow \mathbf{W}^{-1/2}(\Gamma) \times \mathbf{W}^{-1/2}(\Gamma)$ is given by

$$\mathcal{C} := \begin{pmatrix} \frac{1}{2}\mathbf{I} + \mathbf{C}_k & \mathbf{S}_k \\ \mathbf{S}_k & \frac{1}{2}\mathbf{I} + \mathbf{C}_k \end{pmatrix} = \begin{pmatrix} \gamma_{\mathbf{t}} \Psi_{\text{DL}}^k & \gamma_{\mathbf{t}} \Psi_{\text{SL}}^k \\ \gamma_{\mathbf{t}} \Psi_{\text{SL}}^k & \gamma_{\mathbf{t}} \Psi_{\text{DL}}^k \end{pmatrix},$$

and from the representation formula (2) and the identity (9) we obtain

$$\mathcal{C} \begin{pmatrix} \gamma_{\mathbf{t}}(\mathbf{v}) \\ \gamma_{\mathbf{N}}^k(\mathbf{v}) \end{pmatrix} = \begin{pmatrix} \gamma_{\mathbf{t}}(\mathbf{v}) \\ \gamma_{\mathbf{N}}^k(\mathbf{v}) \end{pmatrix}, \quad \mathbf{v} \in \mathbf{H}(\mathbf{curl}^2, \Omega).$$

This yields the boundary integral equations for the Dirichlet and Neumann problems. E.g., for given Dirichlet data $\mathbf{f} \in \mathbf{W}^{-1/2}(\Gamma)$, the Neumann data $\boldsymbol{\sigma} = \gamma_{\mathbf{N}}^k(\mathbf{u}) \in \mathbf{W}^{-1/2}(\Gamma)$ is determined by the equation

$$\mathbf{S}_k(\boldsymbol{\sigma}) = \left(\frac{1}{2}\mathbf{I} - \mathbf{C}_k \right) (\mathbf{f}). \quad (10)$$

Existence and uniqueness of the solution (if k^2 is not an eigenvalue) is established in [4, Sect. 6].

3. The boundary element method for Maxwell's equations

The boundary element method is a Galerkin method for the variational formulation of the integral equation. For the Dirichlet problem (10) this reads as follows: find $\boldsymbol{\sigma} \in \mathbf{W}^{-1/2}(\Gamma)$ such that

$$\langle \mathbf{S}_k(\boldsymbol{\sigma}), \boldsymbol{\chi} \rangle_{\tau, \Gamma} = \langle \frac{1}{2}\mathbf{f} - \mathbf{C}_k(\mathbf{f}), \boldsymbol{\chi} \rangle_{\tau, \Gamma}, \quad \boldsymbol{\chi} \in \mathbf{W}^{-1/2}(\Gamma).$$

For a given subspace $\mathbf{W}_h^{-1/2}(\Gamma) \subset \mathbf{W}^{-1/2}(\Gamma)$ find $\boldsymbol{\sigma}_h \in \mathbf{W}_h^{-1/2}(\Gamma)$ such that

$$\langle \mathbf{S}_k(\boldsymbol{\sigma}_h), \boldsymbol{\chi}_h \rangle_{\tau, \Gamma} = \langle \frac{1}{2}\mathbf{f} - \mathbf{C}_k(\mathbf{f}), \boldsymbol{\chi}_h \rangle_{\tau, \Gamma}, \quad \boldsymbol{\chi}_h \in \mathbf{W}_h^{-1/2}(\Gamma).$$

Introducing a numbering of the boundary element basis $\boldsymbol{\Phi}_1, \dots, \boldsymbol{\Phi}_N$ we obtain the stiffness matrix and the right-hand side (using Lem. 1 for the evaluation of the integral operators)

$$A(k) \approx \left(\langle \mathbf{S}_k(\boldsymbol{\Phi}_n), \boldsymbol{\Phi}_m \rangle_{\tau, \Gamma} \right)_{n, m=1, \dots, N}, \quad b(k) \approx \left(\langle \frac{1}{2}\mathbf{f} - \mathbf{C}_k(\mathbf{f}), \boldsymbol{\Phi}_n \rangle_{\tau, \Gamma} \right)_{n=1, \dots, N},$$

where we compute all singular integrals approximately with the transformation technique in [13, Chap. 5]. Then, if $\xi \in \mathbb{C}^N$ solves $A(k)\xi = b(k)$, the boundary element solution is given by $\boldsymbol{\sigma}_h = \sum_n \xi_n \boldsymbol{\Phi}_n$. Note that for real data all computations can be restricted to the real part.

If k^2 is not an eigenvalue of the continuous problem, a mesh size h_0 exists such that for $h < h_0$ the finite element matrix $A(k)$ is regular [4, Sect. 9].

3.1. A boundary element discretization

We assume that Γ is a polygonal boundary, and let Γ_h be a triangulation into triangles Γ_j . Moreover, let Ω_h be a tetrahedral mesh with boundary Γ_h , and let \mathcal{E}_h be the edges of the boundary triangulation.

Let $\widehat{\Gamma}$ be the reference triangle. The Raviart-Thomas elements $(\widehat{\Gamma}, \mathbf{P}_{\widehat{\Gamma}}, \Sigma_{\widehat{\Gamma}})$ of degree l use the polynomial ansatz space $\mathbf{P}_{\widehat{\Gamma}} := \mathbb{P}_l^2 \oplus \widetilde{\mathbb{P}}_l x$. Here, we only consider the lowest order case $l = 0$. Then, the degrees of freedom are the functionals $\widehat{\boldsymbol{\Phi}}'_e \in \Sigma_{\widehat{\Gamma}} \subset \mathbf{P}'_{\widehat{\Gamma}}$ defined by the flux across the edges

$$\langle \widehat{\boldsymbol{\Phi}}'_e, \widehat{\mathbf{v}} \rangle = \int_{\widehat{e}} \widehat{\mathbf{v}} \cdot \widehat{\mathbf{n}}_e \, d\widehat{l}, \quad \widehat{\mathbf{v}} \in \mathbf{P}_{\widehat{\Gamma}},$$

where $\widehat{e} \subset \partial\widehat{\Gamma}$ is an edge with normal $\widehat{\mathbf{n}}_e$. Let $\widehat{\boldsymbol{\Phi}}_e \in \mathbf{P}_{\widehat{\Gamma}}$ be the associated basis function, i.e., $\langle \widehat{\boldsymbol{\Phi}}'_e, \widehat{\boldsymbol{\Phi}}_e \rangle = 1$ and $\langle \widehat{\boldsymbol{\Phi}}'_e, \widehat{\boldsymbol{\Phi}}_{e'} \rangle = 0$ for $\widehat{e} \neq e'$, see Tab. 1.

edge \widehat{e}	$\text{conv}\{\widehat{z}_0, \widehat{z}_1\}$	$\text{conv}\{\widehat{z}_1, \widehat{z}_2\}$	$\text{conv}\{\widehat{z}_2, \widehat{z}_0\}$
basis function $\widehat{\boldsymbol{\Phi}}_e(\xi, \eta)$	$(\xi, \eta - 1)$	(ξ, η)	$(\xi - 1, \eta)$
$\widehat{\text{div}}\widehat{\boldsymbol{\Phi}}_e$	2	2	2

Table 1: Basis functions for lowest order Raviart-Thomas elements on the reference triangle $\widehat{\Gamma} = \text{conv}\{\widehat{z}_0 = (0, 0), \widehat{z}_1 = (1, 0), \widehat{z}_2 = (0, 1)\}$.

Let $\varphi_j: \widehat{\Gamma} \rightarrow \Gamma_j$ be the linear affine transformation onto a boundary triangle Γ_j , and let $F_j = D\varphi_j$ be the Jacobian and $G_j = F_j^T F_j$ be the associated Gram's matrix. Let $\widehat{e} = \text{conv}\{\widehat{z}_m, \widehat{z}_n\}$ be an edge with unit tangent vector $\widehat{\mathbf{t}}_e = \frac{1}{|\widehat{z}_m - \widehat{z}_n|}(\widehat{z}_m - \widehat{z}_n)$ and outer normal $\widehat{\mathbf{n}}_e$ on $\partial\widehat{\Gamma}$. This defines for the edge $e = \varphi_j(\widehat{e}) \subset \partial\Gamma_j$ the normalized tangent vector $\mathbf{t}_e = \frac{1}{|F_j \widehat{\mathbf{t}}_e|} F_j \widehat{\mathbf{t}}_e$. Now, from $\widehat{\mathbf{t}}_e \cdot \widehat{\mathbf{n}}_e = (F_j \widehat{\mathbf{t}}_e)^T F_j^{-T} \widehat{\mathbf{n}}_e = 0$ we observe that $\mathbf{n}_e = \frac{\text{sign}(e)}{|F_j^{-T} \widehat{\mathbf{n}}_e|} F_j^{-T} \widehat{\mathbf{n}}_e \in \text{affine}(\Gamma_j)$ is the tangential normal vector. Here, the direction of the tangential normal

at $e = \partial\Gamma_j \cap \partial\Gamma_m$ depends on the orientation, where we choose $\text{sign}(e) = 1$ if $j < m$ and -1 else.

For the construction of the discrete space $\mathbf{W}_h^{-1/2}(\Gamma)$ we define the degrees of freedom by

$$\langle \Phi'_e, \mathbf{v} \rangle = \int_e \mathbf{v} \cdot \mathbf{n}_e \, dl, \quad \mathbf{v} \in \mathbf{P}_{\Gamma_j}.$$

We obtain by direct calculus

$$|F_j \widehat{\mathbf{t}}_e|^2 = |\det(F_j) F_j^{-T} \widehat{\mathbf{n}}_e|^2 = \det(G_j) |F_j G_j^{-1} \widehat{\mathbf{n}}_e|^2,$$

which gives $|F_j \widehat{\mathbf{t}}_e| \mathbf{n}_e = \text{sign}(e) \sqrt{\det(G_j)} F_j G_j^{-1} \widehat{\mathbf{n}}_e$ and preserves normal components up to scaling by the evaluation

$$\begin{aligned} \langle \Phi'_e, \mathbf{v} \rangle &= \int_{\widehat{e}} (\mathbf{v} \circ \varphi_j) \cdot \mathbf{n}_e |F_j \widehat{\mathbf{t}}_e| \, d\widehat{l} \\ &= \text{sign}(e) \int_{\widehat{e}} (\mathbf{v} \circ \varphi_j) \cdot (\sqrt{\det(G_j)} F_j G_j^{-1} \widehat{\mathbf{n}}_e) \, d\widehat{l} \\ &= \text{sign}(e) \int_{\widehat{e}} (\sqrt{\det(G_j)} G_j^{-1} F_j^T \mathbf{v} \circ \varphi_j) \cdot \widehat{\mathbf{n}}_e \, d\widehat{l}. \end{aligned}$$

Thus, the boundary element basis function Φ_e defined by duality to the degrees of freedom satisfies $\text{sign}(e) \sqrt{\det(G_j)} G_j^{-1} F_j^T \Phi_e \circ \varphi_j = \widehat{\Phi}_e$, i.e.,

$$\Phi_e \circ \varphi_j = \text{sign}(e) \left(\sqrt{\det(G_j)} \right)^{-1} F_j \widehat{\Phi}_e.$$

Moreover, since $\text{div} \mathbf{P}_{\widehat{\Gamma}} \in \mathbb{P}_0$, we obtain from

$$\begin{aligned} \int_{\widehat{\Gamma}} (\text{div}_{\Gamma} \Phi_e \circ \varphi_j) \sqrt{\det(G_j)} \, d\widehat{s} &= \int_{\Gamma_j} \text{div}_{\Gamma} \Phi_e \, ds = \sum_{e \in \Gamma_j} \int_e \Phi_e \cdot \mathbf{n}_e \, dl \\ &= \sum_{\widehat{e} \in \widehat{\Gamma}} \int_{\widehat{e}} \widehat{\Phi}_e \cdot \widehat{\mathbf{n}}_e \, d\widehat{l} = \int_{\widehat{\Gamma}} \widehat{\text{div}}_{\widehat{\Gamma}} \widehat{\Phi}_e \, d\widehat{s} \end{aligned}$$

the explicit relation

$$\text{div}_{\Gamma} \Phi_e \circ \varphi_j = \left(\sqrt{\det(G_j)} \right)^{-1} \widehat{\text{div}}_{\widehat{\Gamma}} \widehat{\Phi}_e.$$

Together, this defines the Raviart-Thomas boundary element space by

$$\begin{aligned}\mathbf{W}_h^{-1/2}(\Gamma) &= \text{span} \{ \Phi_e : e \in \mathcal{E}_h \} \\ &= \left\{ \mathbf{v} \in \mathbf{W}^{-1/2}(\Gamma) : G_j^{-1} F_j^T \mathbf{v} \circ \varphi_j \in \mathbf{P}_{\hat{\Gamma}} \text{ for all } j \right\}.\end{aligned}$$

Alternatively, using the identity (3), one can characterize $\mathbf{W}_h^{-1/2}(\Gamma) = \gamma_{\mathbf{t}}(\mathbf{V}_h(\Omega))$ as the trace of the lowest order Nédélec space $\mathbf{V}_h(\Omega) \subset \mathbf{H}(\text{curl}, \Omega)$.

3.2. A numerical test for the boundary value problem

The matrix $A(k)$ and the vector $b(k)$ are assembled in parallel in the finite element code M++ [19, 18], and the resulting equation is solved by a direct solver for dense matrices. We test the method for the unit cube $\Omega = (0, 1)^3$ with $k = 1$ and given solution

$$\mathbf{u}(x) = \begin{pmatrix} x_2 \cos(x_3) + x_3 \cos(x_2) \\ x_1 \cos(x_3) + x_3 \cos(x_1) \\ x_1 \cos(x_2) + x_2 \cos(x_1) \end{pmatrix} \quad (11)$$

by prescribing the corresponding boundary data for the Dirichlet and the Neumann case, respectively.

We use a sequence of meshes obtained by regular refinement with mesh size $h_m = 2^{-m} h_0$ and number of degrees of freedom $N_m = \dim W_{h_m}^{-1/2}(\Gamma)$. The boundary element solution of the Dirichlet problem on refinement level m is denoted by $\sigma_m \in W_{h_m}^{-1/2}(\Gamma)$ and the solution of the Neumann problem by $\varphi_m \in W_{h_m}^{-1/2}(\Gamma)$. The error $\sigma_m - \gamma_{\mathbf{N}}^k(\mathbf{u})$ and $\varphi_m - \gamma_{\mathbf{t}}(\mathbf{u})$, respectively, is measured in $\mathbf{L}_{\mathbf{t}}^2(\Gamma)$, and the convergence rate is estimated by the logarithmic reduction factors $\eta_m^{\text{D}} = \log_2 \frac{\|\sigma_{m-1} - \gamma_{\mathbf{N}}^k(\mathbf{u})\|}{\|\sigma_m - \gamma_{\mathbf{N}}^k(\mathbf{u})\|}$ and $\eta_m^{\text{N}} = \log_2 \frac{\|\varphi_{m-1} - \gamma_{\mathbf{t}}(\mathbf{u})\|}{\|\varphi_m - \gamma_{\mathbf{t}}(\mathbf{u})\|}$. The results for level $m = 0, \dots, 4$ are presented in Tab. 2. One clearly observes linear convergence for the lowest order Raviart-Thomas elements in both cases, which is the expected rate predicted by the a priori analysis in [4, Sect. 9].

m	N_m	$\ \boldsymbol{\sigma}_m - \gamma_{\mathbf{N}}^k(\mathbf{u})\ $	η_m^D	$\ \boldsymbol{\varphi}_m - \gamma_{\mathbf{t}}(\mathbf{u})\ $	η_m^N
0	36	0.52560		0.69761	
1	144	0.26011	1.01484	0.27707	1.33217
2	576	0.13016	0.99884	0.13268	1.06230
3	2304	0.06476	1.00711	0.06489	1.03188
4	9216	0.03225	1.00580	0.03212	1.01452

Table 2: Convergence of the boundary element method for the Maxwell Dirichlet problem (left) and the Maxwell Neumann problem (right).

4. A domain decomposition method

The coupling of different materials can be realized by a domain decomposition approach, where in every subdomain the boundary element method is used and the full problem arises from suitable interface conditions.

Let $\bar{\Omega} = \bigcup_{p=1}^P \bar{\Omega}_p$ be a decomposition into open and non-overlapping subdomains Ω_p with constant permittivity ε_p and permeability μ_p , and we set $\beta_p = \sqrt{\varepsilon_p/\mu_p}$. Let $\Gamma = \partial\Omega$, $\Gamma_p = \partial\Omega_p$, $\Gamma_{pq} = \Gamma_p \cap \Gamma_q$, and let $\Gamma_I = \bigcup_{p < q} \Gamma_{pq}$ be the skeleton of inner boundaries. Set $\Gamma_S = \Gamma_I \cup \Gamma$.

Again, we aim for monochromatic solutions with fixed frequency ω . This corresponds to the wave number $k_p = \omega\sqrt{\varepsilon_p\mu_p}$ on Ω_p . We consider Maxwell's equations for \mathbf{u}^p

$$\nabla \times \nabla \times \mathbf{u}^p - k_p^2 \mathbf{u}^p = \vec{0} \quad \text{and} \quad \nabla \cdot \mathbf{u}^p = 0 \quad (12)$$

in the subdomains Ω_p , the conditions

$$\gamma_{\mathbf{t}}^p(\mathbf{u}^p) + \gamma_{\mathbf{t}}^q(\mathbf{u}^q) = \mathbf{0} \quad (13a)$$

$$\beta_p \gamma_{\mathbf{N}}^{k_p, p}(\mathbf{u}^p) + \beta_q \gamma_{\mathbf{N}}^{k_q, q}(\mathbf{u}^q) = \mathbf{0} \quad (13b)$$

on the interfaces Γ_{pq} , and the Dirichlet boundary condition on the boundary Γ

$$\gamma_{\mathbf{t}}(\mathbf{u}) = \mathbf{f}. \quad (14)$$

For $\boldsymbol{\varphi}^p = \gamma_{\mathbf{t}}^p(\mathbf{u}^p)$ and $\boldsymbol{\sigma}^p = \gamma_{\mathbf{N}}^{k_p, p}(\mathbf{u}^p)$ the Calderon projection yields

$$\begin{pmatrix} \boldsymbol{\varphi}^p \\ \boldsymbol{\sigma}^p \end{pmatrix} = \begin{pmatrix} \frac{1}{2}\mathbf{I} + \mathbf{C}_{k^p}^{\Gamma_p} & \mathbf{S}_{k^p}^{\Gamma_p} \\ \mathbf{S}_{k^p}^{\Gamma_p} & \frac{1}{2}\mathbf{I} + \mathbf{C}_{k^p}^{\Gamma_p} \end{pmatrix} \begin{pmatrix} \boldsymbol{\varphi}^p \\ \boldsymbol{\sigma}^p \end{pmatrix}. \quad (15)$$

4.1. The boundary integral formulation the interface problem

Here we transfer the method proposed in [11] to the Maxwell system. For given Dirichlet data on $\Gamma = \partial\Omega$, we have to compute the Dirichlet trace on the skeleton $\boldsymbol{\varphi} = (\boldsymbol{\varphi}^{pq})_{p<q} \in \mathbf{W}^{-1/2}(\Gamma_I) = \prod_{p<q} \mathbf{W}^{-1/2}(\Gamma_{pq})$ and in every subdomain the Neumann trace $\boldsymbol{\sigma} = (\boldsymbol{\sigma}^p) \in \prod_p \mathbf{W}^{-1/2}(\Gamma_p)$. We define $\boldsymbol{\varphi}^p$ by $\boldsymbol{\varphi}^p|_{\Gamma_{pq}} = \boldsymbol{\varphi}^{pq}$ for $p < q$, $\boldsymbol{\varphi}^p|_{\Gamma_{pq}} = -\boldsymbol{\varphi}^{pq}$ for $p > q$, and $\boldsymbol{\varphi}^p|_{\Gamma} = 0$, and we extend the Dirichlet boundary data \mathbf{f} to the skeleton by $\mathbf{f}|_{\Gamma_I} = 0$.

On the inner skeleton Γ_I , the interface conditions (13a) are fulfilled by construction. From the first equation in (15) we obtain

$$\left\langle \left(\frac{1}{2}\mathbf{I} - \mathbf{C}_{kp}^{\Gamma_p}\right)(\boldsymbol{\varphi}^p), \boldsymbol{\tau}^p \right\rangle_{\tau, \Gamma_p} + \left\langle \mathbf{S}_{kp}^{\Gamma_p}(\boldsymbol{\sigma}^p), \boldsymbol{\tau}^p \right\rangle_{\tau, \Gamma_p} = -\left\langle \left(\frac{1}{2}\mathbf{I} - \mathbf{C}_{kp}^{\Gamma_p}\right)(\mathbf{f}), \boldsymbol{\tau}^p \right\rangle_{\tau, \Gamma_p}$$

for all $\boldsymbol{\tau}^p \in \mathbf{W}^{-1/2}(\Gamma_p)$, and $\text{sign}_p = 1$ if $\boldsymbol{\varphi}^p = \boldsymbol{\varphi}$ and -1 else. On the interface Γ_I , the second equation in (15) together with (13b) yields for all $\boldsymbol{\chi} = (\boldsymbol{\chi}^{pq})_{p<q} \in \mathbf{W}^{-1/2}(\Gamma_I)$

$$\begin{aligned} & \sum_{p<q} \left(\left\langle (\beta_p \mathbf{S}_{kp}^{\Gamma_p} - \beta_q \mathbf{S}_{kq}^{\Gamma_q})(\boldsymbol{\varphi}^{pq}), \boldsymbol{\chi}^{pq} \right\rangle_{\tau, \Gamma_{pq}} \right. \\ & \quad \left. + \left\langle \beta_p \left(\frac{1}{2}\mathbf{I} + \mathbf{C}_{kp}^{\Gamma_p}\right)(\boldsymbol{\sigma}^p) + \beta_q \left(\frac{1}{2}\mathbf{I} + \mathbf{C}_{kq}^{\Gamma_q}\right)(\boldsymbol{\sigma}^q), \boldsymbol{\chi}^{pq} \right\rangle_{\tau, \Gamma_{pq}} \right) \\ & \quad = - \sum_{p<q} \left\langle (\beta_p \mathbf{S}_{kp}^{\Gamma_p} + \beta_q \mathbf{S}_{kq}^{\Gamma_q})(\mathbf{f}), \boldsymbol{\chi}^{pq} \right\rangle_{\tau, \Gamma_{pq}}. \end{aligned}$$

Together, this defines a bilinear form $a(\cdot, \cdot)$ and a right-hand side $\ell(\cdot)$ so that the interface problem has the form

$$a((\boldsymbol{\varphi}, \boldsymbol{\sigma}), (\boldsymbol{\chi}, \boldsymbol{\tau})) = \ell((\boldsymbol{\chi}, \boldsymbol{\tau})), \quad (\boldsymbol{\chi}, \boldsymbol{\tau}) \in \mathbf{W}^{-1/2}(\Gamma_I) \times \prod_p \mathbf{W}^{-1/2}(\Gamma_p).$$

Correspondingly, the discrete interface problem aims to find a boundary element solution $(\boldsymbol{\varphi}_h, \boldsymbol{\sigma}_h) \in \mathbf{W}_h^{-1/2}(\Gamma_I) \times \prod_p \mathbf{W}_h^{-1/2}(\Gamma_p)$ of

$$a((\boldsymbol{\varphi}_h, \boldsymbol{\sigma}_h), (\boldsymbol{\chi}_h, \boldsymbol{\tau}_h)) = \ell((\boldsymbol{\chi}_h, \boldsymbol{\tau}_h)), \quad (\boldsymbol{\chi}_h, \boldsymbol{\tau}_h) \in \mathbf{W}_h^{-1/2}(\Gamma_I) \times \prod_p \mathbf{W}_h^{-1/2}(\Gamma_p).$$

Analogously to [11] it can be shown that the bilinear form (with a suitable scaling) is Hermitian, and a unique solution exists if ω is not an eigenfrequency.

4.2. A numerical test for Maxwell's interface problem

We test the domain decomposition method for a simple configuration with two subdomains with $\Omega_1 = (1/3, 2/3)^3$ and $\Omega_2 = (0, 1)^3 \setminus \overline{\Omega_1}$, i.e., $\Gamma_I = \Gamma_{12}$. For simplicity, we use $k = 1$, $\varepsilon_1 = \varepsilon_2 = 1$, $\mu_1 = \mu_2 = 1$ and the solution (11). For given Dirichlet data on Γ , we have to compute the Dirichlet trace $\varphi_h^I = \varphi_h^{12} \in \mathbf{W}^{-1/2}(\Gamma_I)$ on the interface and the Neumann traces $(\sigma_h^1, \sigma_h^2) \in \mathbf{W}_h^{-1/2}(\Gamma_1) \times \mathbf{W}_h^{-1/2}(\Gamma_2)$ on the subdomain boundaries.

A sequence of meshes with mesh size $h_m = 2^{-m}h_0$ is obtained by regular refinement. Let $N_m = \dim \mathbf{W}_{h_m}^{-1/2}(\Gamma_I) + \dim \mathbf{W}_{h_m}^{-1/2}(\Gamma_1) + \dim \mathbf{W}_{h_m}^{-1/2}(\Gamma_2)$. The results in Tab. 3 clearly show linear convergence as expected, the solution is illustrated in Fig. 1.

m	N_m	$\ \sigma_m^2 - \sigma^2\ $	$\eta_m^{N^2}$	$\ \varphi_m^I - \varphi^I\ $	$\eta_m^{D^2}$	$\ \sigma_m^1 - \sigma^1\ $	$\eta_m^{N^1}$
0	432	0.17426		0.04834		0.01998	
1	1728	0.08609	1.01732	0.02515	0.94266	0.01014	0.97850
2	6912	0.04265	1.01330	0.01268	0.98800	0.00500	1.02006

Table 3: Convergence and logarithmic reduction factor for the Maxwell interface problem with Dirichlet boundary condition.

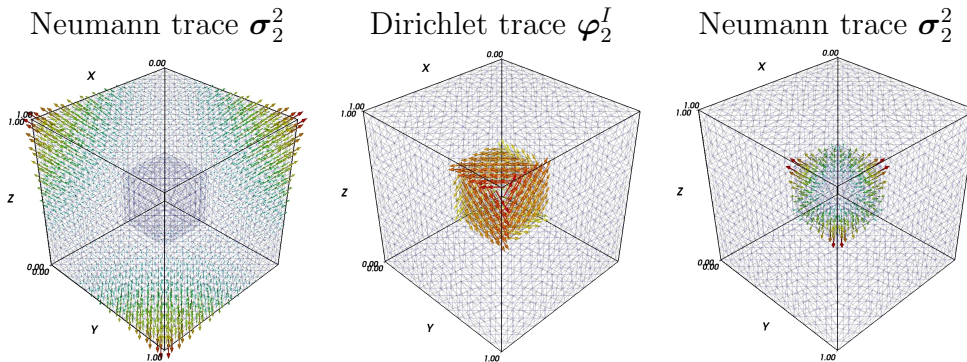


Figure 1: An interface problem for Maxwell's equations with two subdomains.

5. The Maxwell eigenvalue problem

Following the idea proposed by Steinbach and Unger in [15, 17], the boundary element method can be extended to a solution method for the

Maxwell eigenvalue problem: find a non-trivial solution pair (\mathbf{u}, k) of the homogeneous Maxwell system, i.e.,

$$\nabla \times \nabla \times \mathbf{u} + k^2 \mathbf{u}(x) = \mathbf{0} \quad \forall x \in \Omega, \quad (16a)$$

$$\nabla \cdot \mathbf{u}(x) = 0 \quad \forall x \in \Omega, \quad (16b)$$

$$\mathbf{u}(x) \times \mathbf{n} = \mathbf{0} \quad \forall x \in \Gamma. \quad (16c)$$

In order to obtain a unique solution, a suitable normalization of the eigenfunction \mathbf{u} is required.

In terms of boundary integral equations, the Neumann trace $\boldsymbol{\sigma} = \gamma_{\mathbf{N}}^k(\mathbf{u})$ of an eigenpair (\mathbf{u}, k) solving (16) yields a solution $(\boldsymbol{\sigma}, k)$ of the nonlinear problem $\mathbf{S}_k(\boldsymbol{\sigma}) = 0$. This corresponds to the variational problem to find $(\boldsymbol{\sigma}, k) \in \mathbf{W}^{-1/2}(\Gamma) \times \mathbb{R}^+$ with $\boldsymbol{\sigma} \neq 0$ satisfying

$$\langle \mathbf{S}_k(\boldsymbol{\sigma}), \boldsymbol{\chi} \rangle_{\tau, \Gamma} = 0 \quad \forall \boldsymbol{\chi} \in \mathbf{W}^{-1/2}(\Gamma).$$

The Galerkin discretization is to find $(\boldsymbol{\sigma}_h, k_h) \in \mathbf{W}_h^{-1/2}(\Gamma) \times \mathbb{R}^+$ with $\boldsymbol{\sigma}_h \neq 0$ such that

$$\langle \mathbf{S}_{k_h}(\boldsymbol{\sigma}_h), \boldsymbol{\chi}_h \rangle_{\tau, \Gamma} = 0 \quad \forall \boldsymbol{\chi}_h \in \mathbf{W}_h^{-1/2}(\Gamma). \quad (17)$$

Since $\mathbf{S}(k) = \mathbf{S}_k : \Lambda \subset \mathbb{C} \rightarrow \mathcal{L}(W^{-1/2}(\Gamma), W^{-1/2}(\Gamma))$ is holomorphic and satisfies a generalized Garding inequality, the eigenvalue convergence analysis in [16, 17, Chap. 4] applies, and the results for the Helmholtz case [17, Chap. 5] transfer to the Maxwell problem. Thus, on uniform meshes we can expect cubic convergence for the approximation of isolated eigenvalues.

5.1. Newton's Method

The matrix realization of (17) together with a normalization yields the Euclidean formulation to find $(\xi, k_h) \in \mathbb{C}^N \times \mathbb{R}$ such that

$$\begin{aligned} A(k_h)\xi &= 0, \\ \hat{\xi}^H \xi - 1 &= 0, \end{aligned}$$

where a suitable fixed vector $\hat{\xi} \in \mathbb{C}^N$ is a priori chosen. Newton's method starts with some initial guess $(\xi^0, k^0) \in \mathbb{C}^N \times \mathbb{R}$. Then, for $n = 0, 1, 2, \dots$, the next iterate $(\xi^{n+1}, k^{n+1}) \in \mathbb{C}^N \times \mathbb{R}$ is computed by

$$A(k^n)(\xi^{n+1} - \xi^n) + (k^{n+1} - k^n)J_A(k^n)\xi^n = -A(k^n)\xi^n, \quad (18a)$$

$$\hat{\xi}^H(\xi^{n+1} - \xi^n) = -\hat{\xi}^H \xi^n + 1, \quad (18b)$$

where the matrix $J_A(k) = \lim_{\delta \rightarrow 0} \frac{1}{\delta} (A(k + \delta) - A(k))$ is the derivative of $A(\cdot)$ with respect to k . Again, this matrix can be assembled from the boundary integral representation of $\partial_k \mathbf{S}_k$ derived from the expression in Lem. 1

$$\begin{aligned} \langle \partial_k \mathbf{S}_k(\mathbf{v}), \mathbf{w} \rangle_{\tau, \Gamma} = & \int_{\Gamma} \int_{\Gamma} \left(\left(\frac{1}{k} \operatorname{div}_{\Gamma} \mathbf{v}(y) \operatorname{div}_{\Gamma} \mathbf{w}(x) - k \mathbf{v}(y) \cdot \mathbf{w}(x) \right) \partial_k E_k(x, y) \right. \\ & \left. - \left(\frac{1}{k^2} \operatorname{div}_{\Gamma} \mathbf{v}(y) \operatorname{div}_{\Gamma} \mathbf{w}(x) + \mathbf{v}(y) \cdot \mathbf{w}(x) \right) E_k(x, y) \right) ds_y ds_x. \end{aligned}$$

Note that the Newton convergence depends extremely sensitive on the starting iterate, so that global convergence or the convergence to a specific eigenvalue requires additional effort.

5.2. The contour integral method

The contour integral method allows to compute all eigenvalues in a prescribed subset of \mathbb{C} . It is based on the observation that $A(k)$ extends to a holomorphic matrix function $A: \mathbb{C} \rightarrow \mathbb{C}^{N \times N}$ with isolated singular points $\lambda \in \mathbb{C}$. Thus, the matrix function $A(z)^{-1}$ is meromorphic. Now, fix $D \subset \mathbb{C}$ such that $A(z)^{-1}$ is regular for $z \in \partial D$, and assume that $\lambda_1, \dots, \lambda_n$ are the eigenvalues in D with normalized eigenvectors $\xi_j \in \mathbb{C}^N$, i.e., $A(\lambda_j) \xi_j = 0$ and $\xi_j^H \xi_j = 1$. If all eigenvalues λ_j are simple, the matrix function $A(z)^{-1}$ admits a representation

$$A(z)^{-1} = \sum_{j=1}^n \frac{1}{z - \lambda_j} \xi_j \xi_j^H + B(z),$$

where $B(z)$ is a holomorphic matrix function in D [1, Thm. 2.4]. The residual theorem yields for the contour integral matrices

$$\begin{aligned} A_0 &:= \frac{1}{2\pi i} \int_{\partial D} A(z)^{-1} R \, dz = \sum_{j=1}^n \xi_j \xi_j^H R, \\ A_1 &:= \frac{1}{2\pi i} \int_{\partial D} z A(z)^{-1} R \, dz = \sum_{j=1}^n \lambda_j \xi_j \xi_j^H R, \end{aligned}$$

where $R \in \mathbb{C}^{N \times n}$ are suitable (random) test matrices such that A_0 and A_1 have full rank. By construction we have $A_1 A_0^+ = \sum_{j=1}^n \lambda_j \xi_j \xi_j^H \in \mathbb{C}^{N \times N}$,

since the pseudo-inverse of A_0^+ is of the form $A_0^+ = \sum_{j=1}^n R^+ \xi_j \xi_j^H$ with $R^+ \in \mathbb{C}^{n \times N}$ satisfying $R^+ R = I_n$. Moreover, we have for the spectrum $\sigma(A_1 A_0^+) = \sigma(A_0^+ A_1) \cup \{0\}$, which shows that $\lambda_1, \dots, \lambda_n$ are the eigenvalues of the small matrix $A_0^+ A_1 \in \mathbb{C}^{n \times n}$.

For simply connected D and a parametrization $\varphi: [0, 2\pi] \rightarrow \partial D$ with $\varphi(0) = \varphi(2\pi)$ we compute approximations

$$A_{0,M} = \frac{1}{iM} \sum_{m=0}^{M-1} \varphi'(t_m) A(\varphi(t_m))^{-1} R, \quad (19a)$$

$$A_{1,M} = \frac{1}{iM} \sum_{m=0}^{M-1} \varphi(t_m) \varphi'(t_m) A(\varphi(t_m))^{-1} R \quad (19b)$$

with equidistant steps $t_m = m/M$. Then, the approximated eigenvalues λ_j can be recovered from $A_{0,M}^+ A_{1,M} \in \mathbb{C}^{n \times n}$, where the pseudo-inverse can be computed via a singular value decomposition of $A_{0,M}$. For more details on the convergence of the method, the case of multiple eigenvalues, and the case of arbitrary dimensions of the test matrix R we refer to [1, Sect. 3.3].

5.3. Numerical results for Maxwell's eigenvalue problem in one domain

A test example. Again, we start with a simple test in $\Omega = (0, 1)^3$ with $\varepsilon = \mu = 1$, where the eigenvalues $k = \pi \sqrt{\kappa_1^2 + \kappa_2^2 + \kappa_3^2}$ with $\kappa_j \in \mathbb{N}_0$ and eigenfunctions

$$\mathbf{u}_k = \begin{pmatrix} a_1 \cos(\kappa_1 \pi x_1) \sin(\kappa_2 \pi x_2) \sin(\kappa_3 \pi x_3) \\ a_2 \sin(\kappa_1 \pi x_1) \cos(\kappa_2 \pi x_2) \sin(\kappa_3 \pi x_3) \\ a_3 \sin(\kappa_1 \pi x_1) \sin(\kappa_2 \pi x_2) \cos(\kappa_3 \pi x_3) \end{pmatrix} \quad (20)$$

with $a_1 \kappa_1 + a_2 \kappa_2 + a_3 \kappa_3 = 0$ are known explicitly. We use the same discretization as in Sect. 3.2. The eigenvalue convergence with respect to the mesh size is estimated by $\eta_m = \log_2 \frac{|k_{m-1} - k|}{|k_m - k|}$, where the eigenvalues of the discrete problem on level m are denoted by k_m (see Fig. 2 for the Neumann trace of the eigenfunctions).

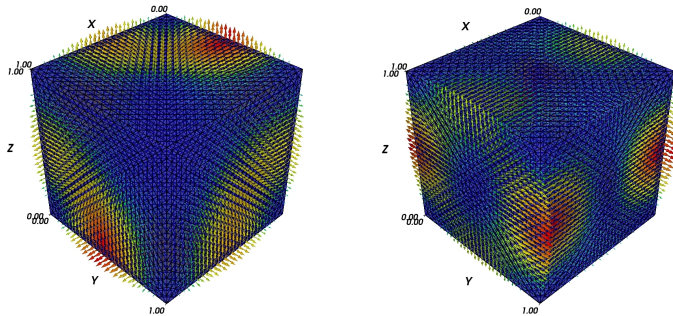


Figure 2: Neumann trace σ_h of the eigenfunctions for the first and second eigenvalue of the problem (17) in the unit cube.

Results for the Newton iteration are presented in Tab. 5 and for the contour integral method in Tab. 6. Both methods approximate k by k_m on level m .

m	N_m	$\kappa = (1, 1, 0)$		$\kappa = (1, 1, 1)$	
		k_m	η_m	k_m	η_m
1	144	4.396130	3.4003	5.319289	3.5230
2	576	4.438455	3.2378	5.430776	3.2216
3	2304	4.442414	3.2957	5.440259	3.2034
4	9216	4.442832		5.441274	
∞		4.442883		5.441398	

Table 4: Discrete eigenvalue convergence of the boundary element method for the test configuration in the unit cube.

As expected from the analysis in [17, Chap. 4] we observe cubic convergence of k_m to k , cf. Tab. 4. Moreover, we observe quadratic convergence for the iterates k_m^n of the Newton steps $n = 1, 2, 3, 4$ in (18), cf. Tab. 5. Here, we find the different eigenvalues by different initial values. This is compared with the contour integral method in Tab. 6, where the first two eigenvalues are approximated simultaneously. The accuracy depends on the discretization parameter M for the evaluation of the approximations $A_{0,M}$ and $A_{1,M}$ in (19) which depends on the discretization level. For this example, the Newton method is more efficient, since a reasonable initial guess can be computed on a coarse mesh. Then, a few Newton steps are sufficient to obtain the

discrete solution, while the contour method requires to assemble more than 20 boundary element matrices to be sufficiently accurate.

	m		step 1	step 2	step 3	step 4
$\kappa = (1, 1, 0)$	1	4	4.406446	4.395935	4.396130	4.396122
	2	4	4.467300	4.437744	4.438455	4.438453
	3	4	4.478139	4.441526	4.442414	4.442411
	4	4	4.480503	4.441905	4.442836	4.442832
$\kappa = (1, 1, 1)$	1	5	5.333690	5.319298	5.319289	5.319289
	2	5	5.469660	5.430716	5.430776	5.430776
	3	5	5.487507	5.440236	5.440259	5.440259
	4	5	5.490671	5.441273	5.441275	5.441274

Table 5: Convergence of the Newton iteration for the approximation of the first and second eigenvalue on level m .

m	$\kappa = (1, 1, 0)$ $k = 4.442883$			$\kappa = (1, 1, 1)$ $k = 5.441398$		
	$M = 10$	$M = 20$	$M = 40$	$M = 10$	$M = 20$	$M = 40$
1	4.396122	4.396106	4.396106	5.313493	5.319359	5.319359
2	4.438467	4.438454	4.438455	5.432038	5.430647	5.430777
3	4.442305	4.442380	4.442414	5.447252	5.440236	5.440259

Table 6: Contour integral method for the test example in the unit cube, where $D \subset \mathbb{C}$ contains the first two eigenvalues, and where ∂D is approximated by a polygon with M segments.

A benchmark problem. Next we compare different finite element approximations and the boundary element approach for a well-known benchmark problem, Maxwell's eigenvalue problem for the Fichera cube $\Omega = (-1, 1)^3 \setminus [0, 1]^3$, see Fig. 3. Here, no analytical solution is available (some reference values are collected in Tab. 7).

	M. Durufé	S. Zaglmayr	IGA ($q = 3$)	IGA ($q = 5$)
λ_1	3.21987401386	3.21999388904	3.21943057045	3.21720448084
λ_2	5.88041891178	5.88044248619	5.88046040750	5.88058776744
λ_3	5.88041891780	5.88045528405	5.88046040842	5.88058776745
λ_4	10.6854921311	10.6856632462	10.6866213844	10.6881376444
λ_5	10.6937829409	10.6936955486	10.6949642900	10.6979155528
λ_6	10.6937829737	10.6937289163	10.6949642906	10.6979155528
λ_7	12.3165204656	12.3168796291	12.3179492061	12.3159290944
λ_8	12.3165204669	12.3176900965	12.3179492065	12.3159290944

Table 7: Reference values for the Maxwell eigenvalues for the Fichera corner from [21, 10, 7].

The results with less than 10 000 degrees of freedom obtained with the boundary element method are already quite close to the reference values (cf. Tab. 8). For the same accuracy, more than 1 000 000 degrees of freedom are required for finite element computations with lowest order elements on uniform meshes, cf. Tab. 9 and 10.

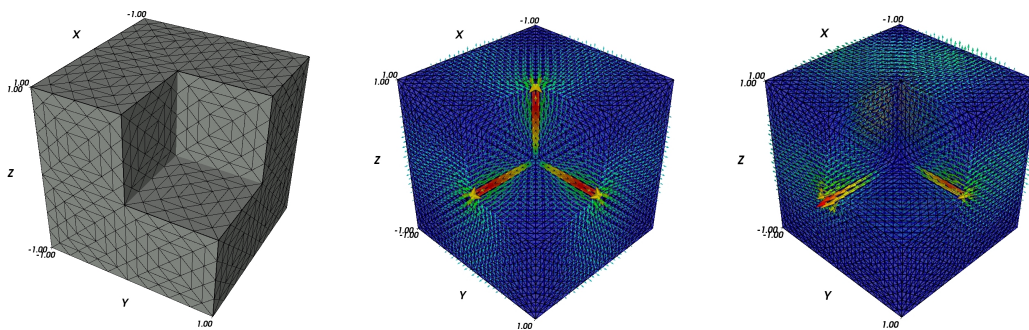


Figure 3: Surface mesh on level 2 for the Fichera corner (left) and Neumann trace σ_h of the first and second eigenvector.

dof	576	2 304	9 216
λ_1	3.2280695	3.2251952	3.2223595
λ_2	5.8548203	5.8764043	5.8795235
λ_3	5.8548412	5.8764080	5.8797125
λ_4	10.5418958	10.6589381	10.6773519
λ_5	10.5817928	10.6670787	10.6853442
λ_6	10.5818145	10.6674636	10.6853942
λ_7	12.2377402	12.3050465	12.3144923
λ_8	12.2378382	12.3051555	12.3157028

Table 8: Boundary element approximations on the Fichera cube.

Here, the contour integral method is more efficient for the boundary element method, since the smallest 8 eigenvalues are computed simultaneously.

The finite element results are obtained by a block iteration with multi-grid preconditioning, see [12] for details. The eigenvalue convergence for the uniform finite element discretization is limited by the regularity of the eigenfunctions; we obtain at most quadratic convergence. For the boundary element discretization again better convergence is observed.

dof	13 720	105 008	821 344	6 496 448	51 675 520
λ_1	3.1171459	3.1814903	3.2053136	3.2142846	3.21771357
λ_2	5.8822584	5.8807766	5.8804931	5.8804338	5.88042136
λ_3	5.8862376	5.8815864	5.8806502	5.8804635	5.88042683
λ_4	10.7361369	10.7021916	10.6912510	10.6875704	10.68626082
λ_5	10.7767298	10.7257200	10.7064673	10.6988093	10.69576043
λ_6	10.8046850	10.7314936	10.7075544	10.6990047	10.69579461
λ_7	12.2978374	12.3052278	12.3111027	12.3141269	12.31550075
λ_8	12.3168109	12.3087798	12.3117339	12.3142344	12.31551839

Table 9: Finite element approximations on tetrahedral meshes.

dof	12 336	92 256	712 896	5 603 712	44 434 176
λ_1	3.1929332	3.2081781	3.2149844	3.2178785	3.21907530
λ_2	5.9044888	5.8867626	5.8821394	5.8809027	5.88056085
λ_3	5.9044888	5.8867626	5.8821394	5.8809027	5.88056085
λ_4	10.8214832	10.7242918	10.6971777	10.6891996	10.68672148
λ_5	10.8380828	10.7374513	10.7078085	10.6985195	10.69544315
λ_6	10.8380828	10.7374513	10.7078085	10.6985195	10.69544315
λ_7	12.4435516	12.3468811	12.3235783	12.3180667	12.31681186
λ_8	12.4435517	12.3468811	12.3235783	12.3180667	12.31681186

Table 10: Finite element approximations on hexahedral meshes.

5.4. The interface eigenvalue problem

The domain decomposition method introduced in Sect. 4 easily transfers to the eigenvalue problem: find a frequency ω and a nontrivial solutions \mathbf{u}^p of

$$\nabla \times \nabla \times \mathbf{u}^p - (\omega/c_p)^2 \mathbf{u}^p = \mathbf{0} \quad \text{and} \quad \nabla \cdot \mathbf{u}^p = 0 \quad (21)$$

in every subdomain Ω_p satisfying the interface conditions (13) on all inner boundaries Γ_{pq} and homogeneous Dirichlet boundary conditions $\gamma_t(\mathbf{u}) = \mathbf{0}$. Here, $c_p = 1/\sqrt{\varepsilon_p \mu_p}$ is the local wave speed.

For the special configuration in Sect. 4.2 with one interface Γ_{12} , we have to compute $\omega > 0$ and $(\varphi^{12}, \boldsymbol{\sigma}^1, \boldsymbol{\sigma}^2) \in \mathbf{W}^{-1/2}(\Gamma_{12}) \times \mathbf{W}^{-1/2}(\Gamma_1) \times \mathbf{W}^{-1/2}(\Gamma_2)$ such that

$$\begin{aligned} & \left(\beta_1 \mathbf{S}_{\omega/c_1}^{\Gamma_1} + \beta_2 \mathbf{S}_{\omega/c_2}^{\Gamma_2} \right) (\varphi^{12}) \\ & + \beta_1 \left(\frac{1}{2} \mathbf{I} + \mathbf{C}_{\omega/c_1}^{\Gamma_1} \right) (\boldsymbol{\sigma}_1) + \beta_2 \left(\frac{1}{2} \mathbf{I} + \mathbf{C}_{\omega/c_2}^{\Gamma_2} \right) (\boldsymbol{\sigma}_2) = 0 \quad \text{on } \Gamma_{12}, \\ & \left(\frac{1}{2} \mathbf{I} - \mathbf{C}_{\omega/c_1}^{\Gamma_1} \right) (\varphi^{12}) + \mathbf{S}_{k_1}^{\Gamma_1} \boldsymbol{\sigma}^1 = 0 \quad \text{on } \Gamma_1, \\ & \left(-\frac{1}{2} \mathbf{I} + \mathbf{C}_{\omega/c_2}^{\Gamma_2} \right) (\varphi^{12}) + \mathbf{S}_{k_2}^{\Gamma_2} \boldsymbol{\sigma}^2 = 0 \quad \text{on } \Gamma^2. \end{aligned}$$

This yields in variational form the following boundary element problem: find

$\omega_h > 0$ and $(\varphi_h^{12}, \sigma_h^1, \sigma_h^2) \in \mathbf{W}_h^{-1/2}(\Gamma_{12}) \times \mathbf{W}_h^{-1/2}(\Gamma_1) \times \mathbf{W}_h^{-1/2}(\Gamma_2)$ such that

$$\begin{aligned}
0 = & \beta_1 \langle \mathbf{S}_{\omega_h/c_1}^{\Gamma_1}(\varphi_h^{12}), \chi_h^{12} \rangle_{\tau, \Gamma_{12}} + \beta_2 \langle \mathbf{S}_{\omega_h/c_2}^{\Gamma_2}(\varphi_h^{12}), \chi_h^{12} \rangle_{\tau, \Gamma_{12}} \\
& + \beta_1 \langle \frac{1}{2} \sigma_h^1 + \mathbf{C}_{\omega_h/c_1}^{\Gamma_1}(\sigma_h^1), \chi_h^{12} \rangle_{\tau, \Gamma_{12}} + \beta_2 \langle \frac{1}{2} \sigma_h^2 + \mathbf{C}_{\omega_h/c_2}^{\Gamma_2}(\sigma_h^2), \chi_h^{12} \rangle_{\tau, \Gamma_{12}} \\
& + \langle \frac{1}{2} \varphi_h^{12} - \mathbf{C}_{\omega_h/c_1}^{\Gamma_1}(\varphi_h^{12}), \tau_h^1 \rangle_{\tau, \Gamma_1} + \langle \mathbf{S}_{\omega_h/c_1}^{\Gamma_1}(\sigma_h^1), \tau_h^1 \rangle_{\tau, \Gamma_1} \\
& + \langle -\frac{1}{2} \varphi_h^{12} + \mathbf{C}_{\omega_h/c_2}^{\Gamma_2}(\varphi_h^{12}), \tau_h^2 \rangle_{\tau, \Gamma_2} + \langle \mathbf{S}_{\omega_h/c_2}^{\Gamma_2}(\sigma_h^2), \tau_h^2 \rangle_{\tau, \Gamma_2}
\end{aligned}$$

for all test functions $(\chi_h^{12}, \tau_h^1, \tau_h^2) \in \mathbf{W}_h^{-1/2}(\Gamma_{12}) \times \mathbf{W}_h^{-1/2}(\Gamma_1) \times \mathbf{W}_h^{-1/2}(\Gamma_2)$. Since this problem is Hermitian, also the discrete approximations ω_h are real.

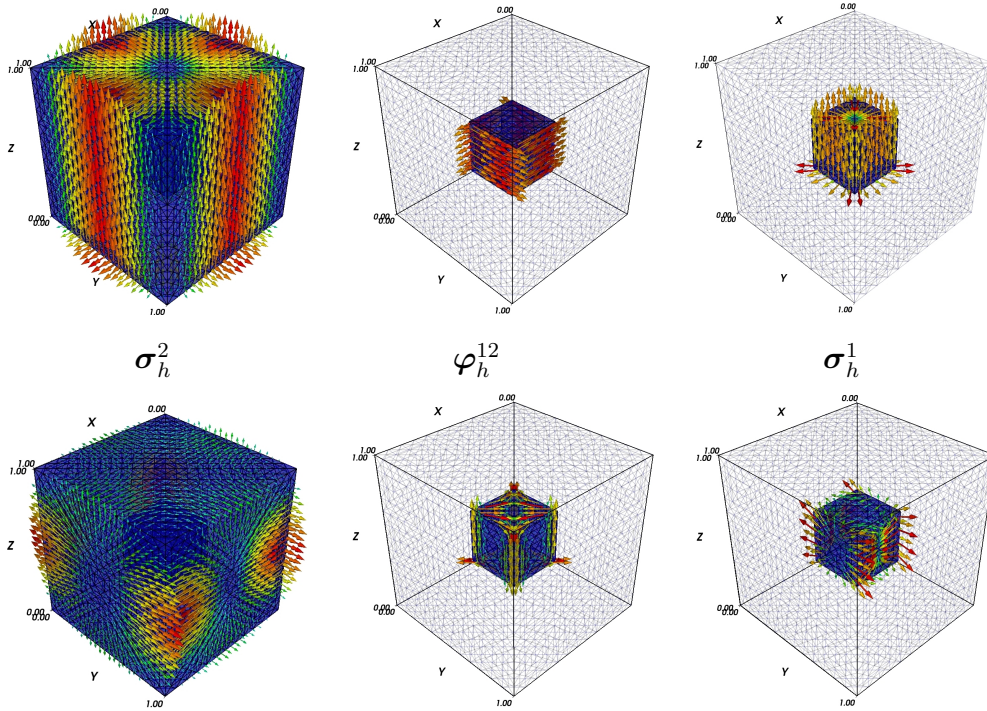


Figure 4: Traces on the subdomain boundaries for the solution of the first and second Maxwell interface eigenvalue problem with homogeneous Dirichlet boundary condition.

In the numerical example we test the convergence for the interface eigenvalue problem using the exact solution (20), see Fig. 4; again, we observe cubic convergence, see Tab. 11.

m	N_m	$\kappa = (1, 1, 0)$			$\kappa = (1, 1, 1)$		
		k_m^{NM}	k_m^{IM}	η_m	k_m^{NM}	k_m^{IM}	η_m
0	432	4.42676	4.42675	3.5593	5.37587	5.37588	3.6474
1	1728	4.44152	4.44152		3.4450	5.43617	
2	6912	4.44276			5.44088		3.3271
∞		4.44288	4.44288		5.44140	5.44140	

Table 11: Eigenvalue convergence for the interface boundary element method. Here, k_m^{NM} and k_m^{IM} are the approximations computed with the Newton method and the contour integral method, respectively.

5.5. Band structure computation for photonic crystals

Finally, we discuss an application to the Maxwell eigenvalue problem on a periodic medium with $\varepsilon(x+z) = \varepsilon(x)$ and $\mu(x+z) = \mu(x)$ for all $z \in \mathbb{Z}^3$. In this case—as a consequence of the Floquet theory—the spectrum of the Maxwell operator is the union of all eigenvalues in the periodicity cell $\Omega = (0, 1)^3$ with quasi-periodic boundary conditions for all $x \in G_j$ ($j = 1, 2, 3$)

$$\gamma_{\mathbf{t}}(\mathbf{u})(x + \mathbf{e}_j) + e^{i\boldsymbol{\alpha} \cdot \mathbf{e}_j} \gamma_{\mathbf{t}}(\mathbf{u})(x) = \mathbf{0}, \quad \gamma_{\mathbf{N}}^k(\mathbf{u})(x + \mathbf{e}_j) + e^{i\boldsymbol{\alpha} \cdot \mathbf{e}_j} \gamma_{\mathbf{N}}^k(\mathbf{u})(x) = \mathbf{0} \quad (22)$$

on the boundary faces $G_1 = [0, 1]^2 \times \{0\}$, $G_2 = [0, 1] \times \{0\} \times [0, 1]$ and $G_3 = \{0\} \times [0, 1]^2$, where \mathbf{e}_j are the unit vectors and $\boldsymbol{\alpha} \in (-\pi, \pi]^3$ is a parameter in the Brillouin zone.

In the periodicity cell, an interface eigenvalue problem has to be solved. We consider an example with $\Omega_1 = (1/8, 7/8)^3$ and $\Omega_2 = (0, 1)^3 \setminus \overline{\Omega_1}$, $\mu_1 = \mu_2 = 1$, $\varepsilon_1 = 1$, and $\varepsilon_2 = 13$. For every $\boldsymbol{\alpha}$ we compute the n lowest frequencies ω_h and $(\boldsymbol{\varphi}_h^{12}, \boldsymbol{\sigma}_h^2|_{\Gamma}, \boldsymbol{\sigma}^2|_{\Gamma_{12}}, \boldsymbol{\varphi}_h^2|_{\Gamma}, \boldsymbol{\sigma}^1) \in \mathbf{W}_h^{-1/2}(\Gamma_{12}) \times \mathbf{W}_h^{-1/2}(\Gamma) \times \mathbf{W}_h^{-1/2}(\Gamma_{12}) \times \mathbf{W}_h^{-1/2}(\Gamma) \times \mathbf{W}_h^{-1/2}(\Gamma_1)$ satisfying the equations (21), the interface conditions (13), and the constraint (22). This leads to the problem to find ω_h such that the matrix of the form

$$\begin{pmatrix} A_{11}(\omega_h) & A_{12}(\omega_h)B_{\boldsymbol{\alpha}} & A_{13}(\omega_h) & A_{14}(\omega_h)B_{\boldsymbol{\alpha}} & A_{15}(\omega_h) \\ B_{\boldsymbol{\alpha}}^H A_{21}(\omega_h) & B_{\boldsymbol{\alpha}}^H A_{22}(\omega_h)B_{\boldsymbol{\alpha}} & B_{\boldsymbol{\alpha}}^H A_{23}(\omega_h) & B_{\boldsymbol{\alpha}}^H A_{24}(\omega_h)B_{\boldsymbol{\alpha}} & 0 \\ A_{31}(\omega_h) & A_{32}(\omega_h)B_{\boldsymbol{\alpha}} & A_{33}(\omega_h) & A_{34}(\omega_h)B_{\boldsymbol{\alpha}} & 0 \\ B_{\boldsymbol{\alpha}}^H A_{41}(\omega_h) & B_{\boldsymbol{\alpha}}^H A_{42}(\omega_h)B_{\boldsymbol{\alpha}} & B_{\boldsymbol{\alpha}}^H A_{43}(\omega_h) & B_{\boldsymbol{\alpha}}^H A_{44}(\omega_h)B_{\boldsymbol{\alpha}} & 0 \\ A_{51}(\omega_h) & 0 & 0 & 0 & A_{55}(\omega_h) \end{pmatrix}$$

is singular, where the constraint (22) is realized by the matrix B_α extending the degrees of freedom on $G_1 \cup G_2 \cup G_3$ to $\Gamma = \partial\Omega$.

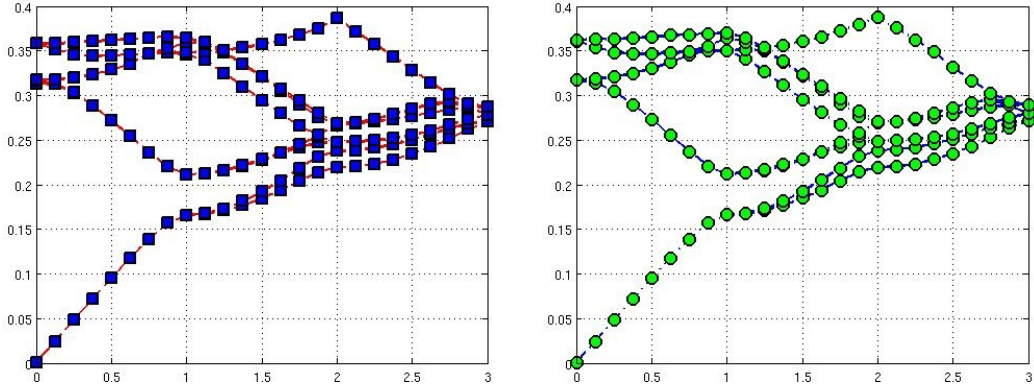


Figure 5: Band structures along a path in the Brillouin zone $(-\pi, \pi]^3$ for a photonic crystal computed with boundary elements (left) and finite elements (right).

The results for the first four bands are presented in Fig. 5, where we compare the eigenvalues for 25 sample points α in the Brillouin zone. Here, the boundary element method can be used efficiently. It is sufficient to assemble the matrices $A_{jl}(z_m)$ ($m = 0, \dots, M - 1$) along the contour. Then, for each sample point α , the full matrix can be easily compiled using B_α , and the four smallest eigenfrequencies can be computed simultaneously. For comparison, we also present the band structure approximation with finite element solution computed with the techniques developed in [8, 20].

Acknowledgments

The authors want to thank G. Unger for his excellent introduction in the results of his PhD thesis and for his suggestion for the comparison with the contour integral method. Moreover, we acknowledge the support of the German Research Foundation and the Research Training Group 1294.

- [1] W. BEYN, *An integral method for solving nonlinear eigenvalue problems*, Linear Algebra Appl., (2011). DOI: 10.1016/j.laa.2011.03.030.
- [2] A. BUFFA, M. COSTABEL, AND C. SCHWAB, *Boundary element methods for Maxwell's equations on non-smooth domains*, Numer. Mathem., 4/92 (2002), pp. 679–710.

- [3] A. BUFFA, M. COSTABEL, AND D. SHEEN, *On traces for $\mathbf{H}(\mathbf{curl}, \Omega)$ for Lipschitz domains*, J. Math. Anal. Appl., 276 (2002), pp. 845–876.
- [4] A. BUFFA AND R. HIPTMAIR, *Galerkin boundary element methods for electromagnetic scattering*, in Computational Methods in Wave Propagation, M. Ainsworth, ed., vol. 31, Springer-Verlag, 2003, pp. 83–124.
- [5] A. BUFFA AND J. P. CIARLET, *On traces for functional spaces related to Maxwell’s equations. Part I: An integration by parts formula in Lipschitz polyhedra*, Math. Meth. Appl. Sci., 21 (2001), pp. 9–30.
- [6] ———, *On traces for functional spaces related to Maxwell’s equations. Part II: Hodge decompositions on the boundary of Lipschitz polyhedra and applications*, Math. Meth. Appl. Sci., 21 (2001), pp. 31–48.
- [7] A. BUFFA, J. RIVAS, G. SANGALLI, AND R. VÁZQUEZ, *Isogeometric discrete differential forms in three dimensions*, SIAM J. Numer. Anal., 49 (2011), pp. 818–844.
- [8] A. BULOVIYATOV, *A parallel multigrid method for band structure computation of 3D photonic crystals with higher order finite elements*, PhD thesis, Karlsruhe Institute of Technology, 2010.
- [9] D. COLTON AND R. KRESS, *Applied Mathematical Sciences*, vol. 93, Springer, Heidelberg, 2 ed., 1998, ch. Inverse Acoustic and Electromagnetic Scattering Theory.
- [10] M. DAUGE, *Benchmark computations for Maxwell equations for the approximation of highly singular solutions*. <http://perso.univ-rennes1.fr/monique.dauge/benchmax.html>.
- [11] U. LANGER, G. OF, O. STEINBACH, AND W. ZULEHNER, *Inexact data-sparse boundary element tearing and interconnecting methods*, SIAM J. Sci. Comput., 29 (2007), pp. 290–314.
- [12] D. MAURER AND C. WIENERS, *Parallel multigrid methods and coarse grid solver for Maxwell’s eigenvalue problem*, in Competence in High Performance Computing, G. W. et. al., ed., Springer, 2012, pp. 205–213.
- [13] S. SAUTER AND C. SCHWAB, *Boundary Element Methods*, Springer-Verlag, Berlin, Heidelberg, 2011.

- [14] O. STEINBACH, *Numerical Approximation Methods for Elliptic Boundary Value Problems. Finite and Boundary Elements*, Springer Science+Business Media, New York, 2008.
- [15] O. STEINBACH AND G. UNGER, *A boundary element method for the dirichlet eigenvalue problem of the laplace operator*, Numer. Math., 113 (2009), pp. 281–298.
- [16] ———, *Convergence analysis of a Galerkin boundary element method for the Dirichlet Laplacian eigenvalue problem*, SIAM J. Numer. Anal., (2012). to appear.
- [17] G. UNGER, *Analysis of Boundary Element Methods for Laplacian Eigenvalue Problems*, phd thesis, TU Graz, 2009.
- [18] C. WIENERS, *Distributed point objects. A new concept for parallel finite elements*, in Domain Decomposition Methods in Science and Engineering, R. Kornhuber, R. Hoppe, J. Périaux, O. Pironneau, O. Widlund, and J. Xu, eds., vol. 40 of Lecture Notes in Computational Science and Engineering, Springer, 2004, pp. 175–183.
- [19] ———, *A geometric data structure for parallel finite elements and the application to multigrid methods with block smoothing*, Journal Computing and Visualization in Science, 13 (2010), pp. 161–175.
- [20] ———, *Calculation of the photonic band structure*, Birkhäuser, New-York, W. Dörfler ed., 2011, pp. 40–62.
- [21] S. ZAGLMAYR, *High order finite element methods for electromagnetic field computation*, PhD thesis, Johannes Kepler University Linz, Austria, 2006.

IWRMM-Preprints seit 2009

- Nr. 09/01 Armin Lechleiter, Andreas Rieder: Towards A General Convergence Theory For Inexact Newton Regularizations
- Nr. 09/02 Christian Wieners: A geometric data structure for parallel finite elements and the application to multigrid methods with block smoothing
- Nr. 09/03 Arne Schneck: Constrained Hardy Space Approximation
- Nr. 09/04 Arne Schneck: Constrained Hardy Space Approximation II: Numerics
- Nr. 10/01 Ulrich Kulisch, Van Snyder : The Exact Dot Product As Basic Tool For Long Interval Arithmetic
- Nr. 10/02 Tobias Jahnke : An Adaptive Wavelet Method for The Chemical Master Equation
- Nr. 10/03 Christof Schütte, Tobias Jahnke : Towards Effective Dynamics in Complex Systems by Markov Kernel Approximation
- Nr. 10/04 Tobias Jahnke, Tudor Udrescu : Solving chemical master equations by adaptive wavelet compression
- Nr. 10/05 Christian Wieners, Barbara Wohlmuth : A Primal-Dual Finite Element Approximation For A Nonlocal Model in Plasticity
- Nr. 10/06 Markus Bürg, Willy Dörfler: Convergence of an adaptive hp finite element strategy in higher space-dimensions
- Nr. 10/07 Eric Todd Quinto, Andreas Rieder, Thomas Schuster: Local Inversion of the Sonar Transform Regularized by the Approximate Inverse
- Nr. 10/08 Marlis Hochbruck, Alexander Ostermann: Exponential integrators
- Nr. 11/01 Tobias Jahnke, Derya Altıntan : Efficient simulation of discret stochastic reaction systems with a splitting method
- Nr. 11/02 Tobias Jahnke : On Reduced Models for the Chemical Master Equation
- Nr. 11/03 Martin Sauter, Christian Wieners : On the superconvergence in computational elastoplasticity
- Nr. 11/04 B.D. Reddy, Christian Wieners, Barbara Wohlmuth : Finite Element Analysis and Algorithms for Single-Crystal Strain-Gradient Plasticity
- Nr. 11/05 Markus Bürg: An hp-Efficient Residual-Based A Posteriori Error Estimator for Maxwell's Equations
- Nr. 12/01 Branimir Anic, Christopher A. Beattie, Serkan Gugercin, Athanasios C. Antoulas: Interpolatory Weighted-H2 Model Reduction
- Nr. 12/02 Christian Wieners, Jiping Xin: Boundary Element Approximation for Maxwell's Eigenvalue Problem

Eine aktuelle Liste aller IWRMM-Preprints finden Sie auf:

www.math.kit.edu/iwrmm/seite/preprints

Kontakt

Karlsruher Institut für Technologie (KIT)
Institut für Wissenschaftliches Rechnen
und Mathematische Modellbildung

Prof. Dr. Christian Wieners
Geschäftsführender Direktor

Campus Süd
Engesserstr. 6
76131 Karlsruhe

E-Mail: Bettina.Haindl@kit.edu

www.math.kit.edu/iwrmm/

Herausgeber

Karlsruher Institut für Technologie (KIT)
Kaiserstraße 12 | 76131 Karlsruhe

März 2012

www.kit.edu